Journal of Biomedical Optics 8(1), 17–25 (January 2003)

In vivo autofluorescence imaging of early cancers in the human tracheobronchial tree with a spectrally optimized system

Didier Goujon
Matthieu Zellweger
Swiss Federal Institute of Technology (EPFL)
Laboratory for Air and Soil Pollution
1015 Lausanne, Switzerland

Alexandre Radu
Pierre Grosjean
CHUV Hospital
ENT Clinic
1011 Lausanne, Switzerland

Bernd-Claus Weber
Richard Wolf Endoskope GmbH
Postfach 1164
D-75434 Knittlingen, Germany

Hubert van den Bergh
Swiss Federal Institute of Technology (EPFL)
Laboratory for Air and Soil Pollution
1015 Lausanne, Switzerland

Philippe Monnier
CHUV Hospital
ENT Clinic
1011 Lausanne, Switzerland

Georges Wagnières
Swiss Federal Institute of Technology (EPFL)
Laboratory for Air and Soil Pollution
1015 Lausanne, Switzerland

Abstract. The changes in the autofluorescence characteristics of the bronchial tissue is of crucial interest as a cancer diagnostic tool. Evidence exists that this native fluorescence or autofluorescence of bronchial tissues changes when they turn dysplastic and to carcinoma *in situ*. There is good agreement that the lesions display a decrease of autofluorescence in the green region of the spectrum under illumination with violet-light, and a relative increase in the red region of the spectrum is often reported. Imaging devices rely on this principle to detect early cancerous lesions in the bronchi. Based on a spectroscopic study, an industrial imaging prototype is developed to detect early cancerous lesions in collaboration with the firm Richard Wolf Endoskope GmbH, Germany. A preliminary clinical trial involving 20 patients with this spectrally optimized system shows that the autofluorescence can help to detect most lesions that would otherwise have remained invisible to an experienced endoscopist under white light illumination. A systematic off line analysis of the autofluorescence images pointed out that real-time decisional functions can be defined to reduce the number of false positive results. Using this method, a positive predictive value (PPV) of 75% is reached using autofluorescence only. Moreover, a PPV of 100% is obtained, when combining the white light (WL) mode and the autofluorescence (AF) mode, at the applied conditions. Furthermore, the sensitivity is estimated to be twice higher in the AF mode than in WL mode. [DOI: 10.1117/1.1528594]

Keywords: photodetection; autofluorescence; early bronchial cancer; decisional thresholds.

Paper 01016 received Feb. 26, 2001; revised manuscript received Feb. 7, 2002; accepted for publication July 9, 2002.

1 Introduction

All biological tissues emit fluorescence when excited by UV or visible light. This fluorescence is emitted by naturally occurring fluorophores and is therefore often called autofluorescence. It was already reported that early cancerous tissues have a different autofluorescence emission spectrum than healthy tissues.[1,2] Although the modifications of the autofluorescence spectra probably originate in the structure of tissues or in metabolic processes,[3,4] the reasons it is observed in early tumors remain controversial and have been widely studied. They can be sorted into two broad categories: biochemical effects and architectural effects. Note also that the nonfluorescing heme also influences the spectral shape of tissue autofluorescence if the heme concentration varies. Therefore, the use of autofluorescence spectral imaging techniques for the characterization of biological tissues remains a pragmatic approach.

Nevertheless, the ensuing contrast between early cancers and healthy tissue has been taken advantage of for detection purposes, eventually leading to the commercialization of several systems (Xillix,[3] Pentax,[5] Storz[6]). However, many spectral features remain suboptimal, and this is the reason why we performed a spectroscopic study of autofluorescence emission of human healthy, metaplastic, and dysplastic carcinoma *in situ* (CIS) bronchial tissue, covering excitation wavelengths from 350 to 480 nm in a separate study.[1]

The measurements were performed with a spectrofluorometer whose distal end was designed to simulate the spectroscopic response of an imaging system using standard bronchoscopes. The data provide information about the excitation and emission spectral ranges to be used in a dual-range detection imaging system to maximize the healthy versus nonhealthy contrast in detecting premalignant and early malignant lesions. We demonstrate that the excitation wavelengths inducing the highest contrasts are found between 400 and 440 nm with a peak at 405 nm, and that the region of divergence between the tumor and the nontumor spectra is consistently between 600 and 800 nm. Moreover the transition wavelength between the two spectral regions is around 590 nm for all the spectra regardless of the excitation wavelength. Based on this spectroscopic study,[1] we developed an imaging system to de-

Address all correspondence to Georges Wagnières. Tel: +41 21 693 31 20; Fax: +41 21 693 36 26; E-mail: Georges.Wagnieres@epfl.ch

1083-3668/2003/$15.00 © 2003 SPIE

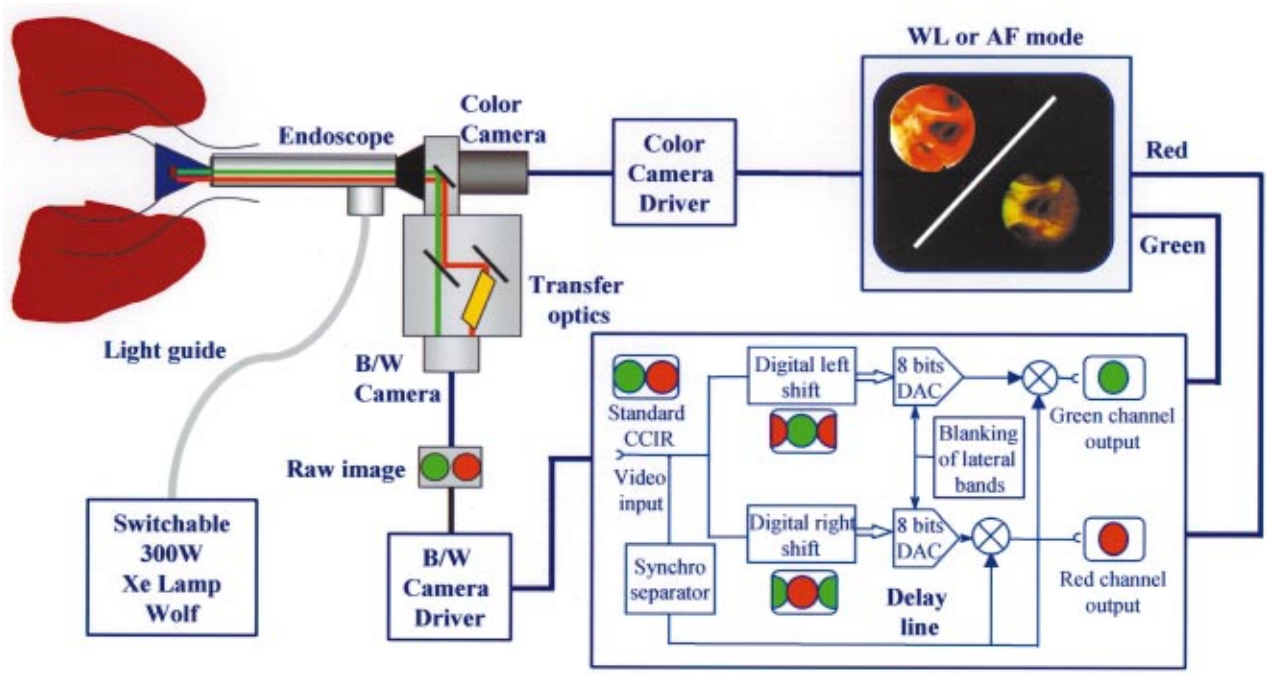

Fig. 1 Diagram of the photodetection apparatus.

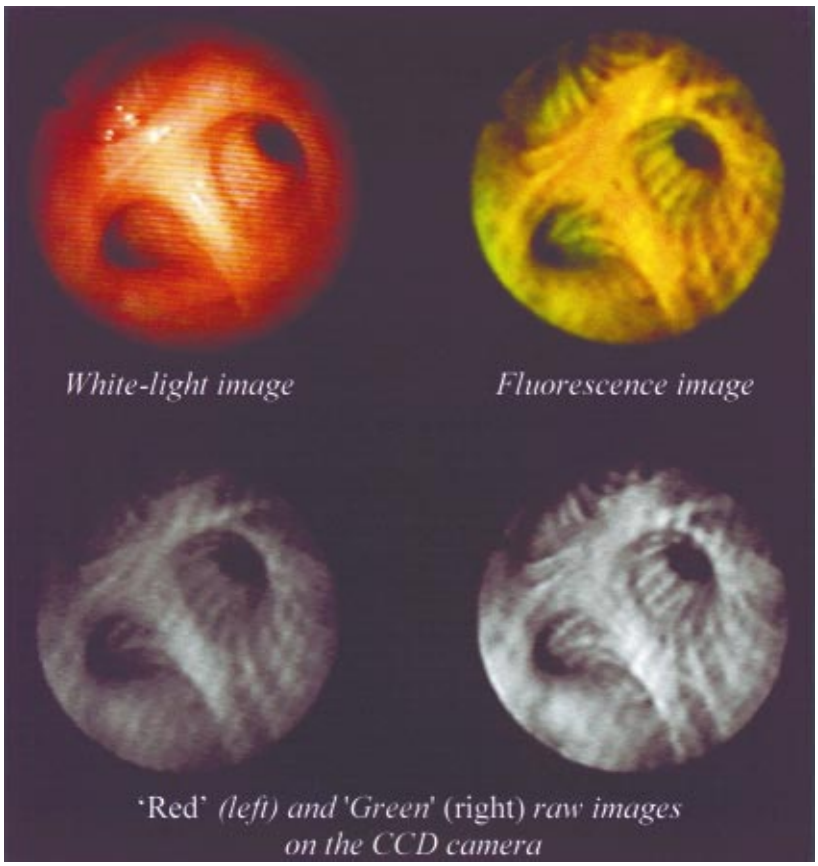

Fig. 2 Photodetection of a healthy tissue with a flexible bronchoscope.

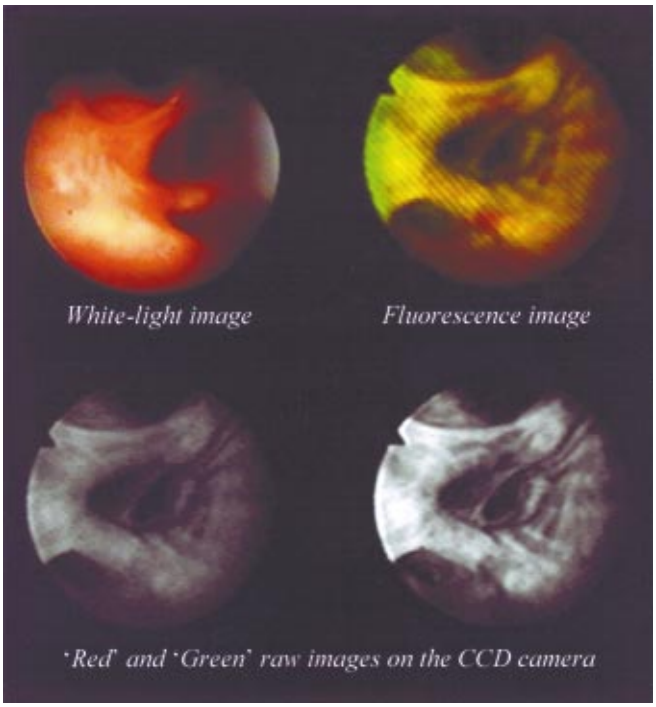

Fig. 3 Photodetection of a low-grade dysplasia on a 62-year-old male patient (flexible bronchoscope).

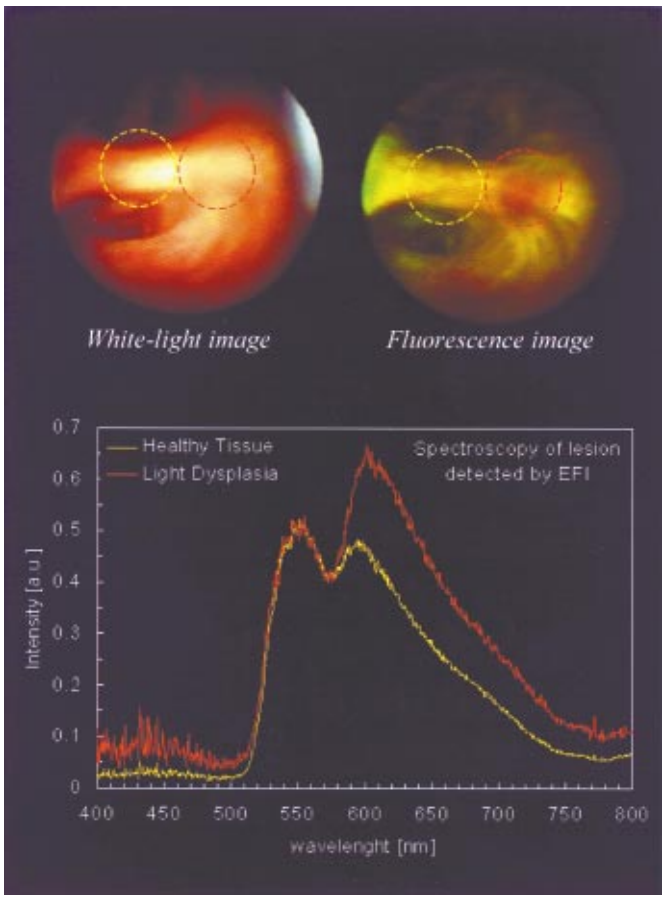

Fig. 4 Photodetection and spectroscopy (spectra are normalized at 550 nm) of a low-grade dysplasia on a 62-year-old male patient (flexible bronchoscope).

tect premalignant and early lesions in the tracheobronchial tree in collaboration with the firm Richard Wolf Endoskope GmbH, Germany.

2 Material and Methods

2.1 Fluorescence Excitation

The excitation of the autofluorescence is achieved by means of a filtered 300-W Xe lamp (5133 Combilight PDD: Wolf Endoskope, Knittlingen, Germany) in the violet-blue range (390 to 460 nm, custom-made filters). The lamp is also equipped with an IR blocking filter. The light is transmitted from the lamp to the endoscope via a liquid light guide (Type 4070.253: Wolf Endoskope, Knittlingen, Germany). The available excitation power at the distal end of a standard rigid bronchoscope (0 deg, Type 8465.30 endoscope: Wolf Endoskope, Knittlingen, Germany) is about 260 mW in the specified spectral range.

A dedicated flexible bronchoscope was also developed for this application (type 7265.006 bronchofiberscope equipped with UV illumination fibers: Wolf Endoskope, Knittlingen, Germany), enabling an excitation power of about 120 mW at its distal end in the same spectral domain.

2.2 Fluorescence Detection

The photodetection system relies on one black and white (B/W) CCD camera (Type: CF 8/1 FMC; Kappa Messtechnik GmbH, Gleichen, Germany) and a dual-detection range: 500 to 590 nm (hereafter the green region) and 600 to 700 nm (hereafter the red region). In fact, at least two spectral domains are necessary for efficient contrast enhancement. However, detection over many spectral regions is shot-noise limited. A device, clipped at the eyepiece of a standard bronchoscope, framed the optical elements to separate the fluorescence light into its color components (dichroic mirror), to filter the unwanted light (long-pass filter, color filters), and to focus the two resulting light streams (one for the green region and one for the red region) on the same microhead B/W CCD camera. The signal was then processed by a delay line, which first duplicated the signal and then delays the two resulting signals (one for the green component and one for the red) from a given amount of time (13 μs for the green component; 51 μs for the red component), thus enabling the superimposition of the two components in false colors on a Sony trinitron color monitor (Type: PVM-2053 MD) (Figure 1). The gain and offset of the delayed signals can also be adjusted individually. The offset was adjusted to zero, and the gain levels of both the red and green images were adapted according to the following procedure. The endoscope was introduced in the trachea and maintained at a typical working distance to the carina. The gain of the red channel was then increased to generate a red image whose brightness corresponded to half the dynamic range of the system. The gain of the green channel was then enhanced to a level resulting in a green-yellowish appearance for the healthy tissues of the carina on the result image. The system was completed with standard VCRs, which enabled the recording of the raw B/W signal and the resulting false color signal. Note that a switchable mirror also enabled observation of the endoscopic site under standard white light illumination with a standard color camera.

Typical autofluorescence (AF) raw fluorescence images (B/W), the processed images and the corresponding white light (WL) image obtained with a flexible bronchoscope on a healthy tissue are presented in Figure 2.

An advantage of this system over existing ones is its ability to work at video frequency (no frame accumulation necessary) and to switch rapidly between the violet and WL illumination. In fact, the AF images are bright enough to enable the clinician to navigate in the tracheobronchial tree with the possibility to rapidly observe a suspicious site in a conventional way. Finally, this system is compact, reliable (no computer is used as long as the threshold calculation described later is not necessary), and relatively inexpensive as it avoids the use of costly devices such as image intensifiers and nonstandard components.

2.3 Patients

Twenty patients with high lung cancer risk factors (positive sputum cytology, positive resection margin following lobectomy, patients within the regular follow-up of lung cancers) underwent WL and AF bronchoscopy. Thirty-three biopsies were taken at macroscopically suspicious (WL or AF positive) and control sites. These biopsies were analyzed using standard procedures by the Histopathology Unit of the Lausanne's CHUV Hospital.

Photodetection took place in the following manner. A first survey of the bronchi was undertaken by the endoscopist under standard WL. This was intended to assess the state of the mucosa and the presence or absence of notable lesions under white light. The bronchi were then examined again under AF excitation light. Care was taken not to damage the mucosa during these examinations. A biopsy was taken on each suspicious WL or AF site and the results were compared to the histopathological analysis. Reddish brown sites under AF light excitation were considered positive and greenish sites negative.

Different AF and WL images corresponding to different histopathological statuses are presented in Figures 3–7. Figure 7 presents a photodetection of an hyperplasia in a 61-year-old male patient. The patient underwent a bronchoscopy because of an extrinsic compression of the lower and middle right lobes. Hyperplasia is not a premalignant or early lesion, but the site appears positive in AF mode (and negative in WL mode). Nevertheless, note that as compared to Figures 3–6, the color aspect of the suspicious area is slightly different: it appears less reddish. This case is a false positive result, if the decisional algorithms presented later are not used.

According to this result, the question of the assessment of the positivity of a site is of crucial interest. One approach is to find a way to quantify the positivity of the AF sites and to define a threshold of positivity. Indeed, some sites appear reddish and some other sites appear more orange-looking and, as we see later, this is correlated to the actual status of the tissue.

Several false positive results occurred during the early stages of our study and hinted at the necessity to quantitatively assess the ''redness'' of a spot and not just rely on the subjective visual assessment of the clinician. This is especially true since we initially lacked quantitative decision criteria and hence sometimes the reddest spot in the bronchi of one patient was assigned a positive result, even though it might have not been considered positive in another patient.

Table 1 Histopathological codes and number of the 33 tissue sites that were biopsied because they were positive under AF and/or WL observation. The epidermoid carcinoma corresponding to the code 7 were local endobronchial invasive carcinoma.

Histopathological Status	Code	Number of Sites
Healthy	1	2
Chronic inflammation	2	6
Mature metaplasia	3	16
Light dysplasia	4	1
Moderate dysplasia	5	1
Severe dysplasia/CIS	6	4
Epidermoid carcinoma	7	3

This demonstrates that a quantitative approach using decision functions is not only useful, but also necessary for maximal efficiency of the method.

2.4 Threshold Approach

We quantified the green and the red contribution in the images taken with our system and then calculated the resulting green/red ratio. These ratios were plotted against the histopathological status of the tissue and the result is given in Figure 8.

The points were calculated in the following way. For each site to be biopsied, an AF image was recorded with our system under broadband violet-blue light excitation. The resulting images were digitized using 8-bit quantification. The average intensity (and the corresponding standard deviation) of the green and red pixels was computed on the site of the biopsy and next to it on presumably healthy tissue. This is the reason why $33 \times 2 = 66$ points are presented in Figure 8. The corresponding green and red intensities were then divided, respectively, by the total green and the total red intensities recorded on one image of presumably healthy tissue to take into account the fact that the green and red gains are set independently for each patient (normalization). The green/red ratio of these normalized green and normalized red contributions was computed, together with its standard deviation and plotted versus the histopathological status of the site as given by the histopathologist. For the sake of the readability of Figure 8, the histopathological status has been coded with a number. These numbers are given in Table 1.

The histopathological status codes have been separated in three groups. Healthy tissues are assigned to the first group (healthy group: green points). Chronic inflammation and metaplasias have been assigned to the second group (nonhealthy group: orange points). This intends to group together the tissue changes that are not malignant. The third group (cancer group: red points) includes the dysplasias and cancers. This grouping could be justified in a system of optical biopsy.

Figure 8 summarizes the quantification of the autofluorescence changes observed during our preliminary study. Each point is given with its standard deviation. This is due to the fact that the color contribution of the green and red components are not fully homogenous. They are fairly stable, however, as we can see in the small error bars. Assuming that these points represent a normal distribution, a curve can be drawn to express it. This has been done for each of the three groups (healthy group, curve 1, group 1; nonhealthy group, curve 2, group 2; cancer group, curve 3, group 3) and is represented in Figure 8 as three projected curves on the left side of the graph. We can see that the three curves are actually separated. Nevertheless, the overlap of the healthy group ($\mu = 1.018$, $\sigma = 0.143$) and the nonhealthy group is nonnegligible and so is also the overlap of the nonhealthy group ($\mu = 0.728$, $\sigma = 0.103$) and the cancer group ($\mu = 0.575$, $\sigma = 0.121$). The aim of such a quantification, however, is to fix an optimal threshold at an objective value to distinguish early cancers from nonmalignant changes. As the curves overlap, it is likely that there will always be some wrong results.

Nevertheless, for our study, the thresholds have been set to the values where the healthy and nonhealthy curves cross for the healthy threshold (value of 0.85) and where the cancer and nonhealthy curves cross for the cancer threshold (value of 0.66). This involves that there is still an error of 25.4% ($= 0.66\ \sigma$) for a nonhealthy case to be in fact a cancer case, as well as an error of 4.9% ($= 1.96\ \sigma$) for a healthy case to be a cancer case, according to this preliminary study. Nevertheless, an analysis based on the positive predictive value (PPV) was performed to evaluate the efficiency of the method.

3 Results

3.1 Illustrations

Figure 3 presents a photodetection of a light dysplasia in a 62-year-old male patient. This patient underwent a bronchoscopy following a positive esophageal cytology (high-grade dysplasia). The presence of low-grade epithelial dysplasia in the bronchi was confirmed by the histopathological analysis. On this patient, we also made a spectroscopic measurement with our spectrofluorometer.[1] For this special measurement, the excitation light used was the broad violet-blue excitation light (390 to 460 nm) of the AF detection device. Two spectroscopic measurements were made: one on the lesion and one on the healthy tissue next to the lesion. The two spectra have been normalized at 550 nm to compare their shape. The resulting spectra are shown on Figure 4, associated with enlarged pictures of the measured area: the red spectrum is associated with the lesion (corresponding to red circles on photos), and the yellow one with the healthy tissue (yellow circles on photos). The decrease of the fluorescence signal intensity in the green region (on the lesion) is therefore seen as an increase in the red one. Moreover, in the raw image (B/W) of Figure 3, one can clearly observe that this intensity decrease in the green region is associated with an intensity decrease in the red region to a lesser extent. This is in full agreement with our spectroscopic observation.[1]

Figures 5 and 6 present a photodetection of a 71-year-old male patient. This patient underwent a control bronchoscopy 4 months after a lobectomy (right upper lobe). He also had undergone a photodynamic therapy[7] (PDT) in the left upper lobe 3 months earlier.

Two suspicious sites were found in the bronchi of this patient, one on the lobectomy scar (Figure 5) and one on the site of the previous PDT (Figure 6). Two biopsies were taken, one on each site. The histopathological analysis of the first

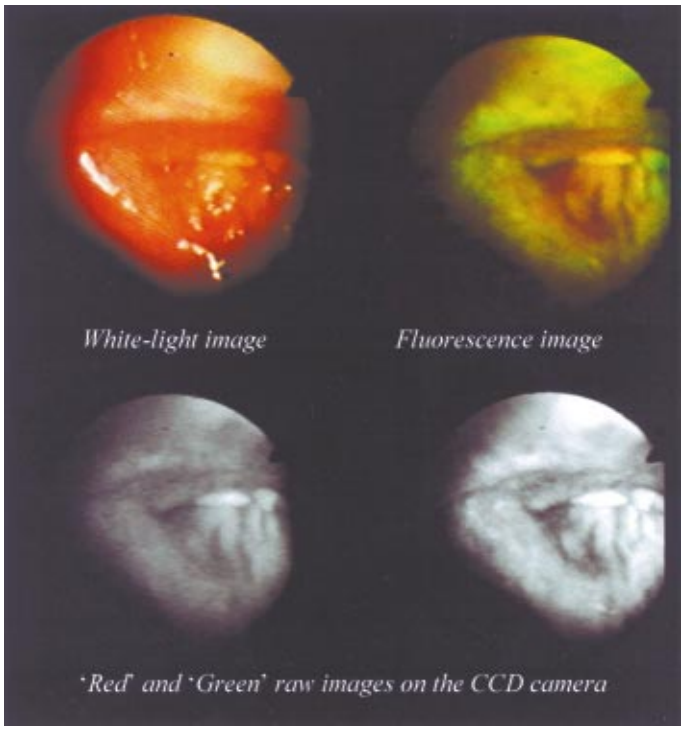

Fig. 5 Photodetection of an infiltrating epidermoid carcinoma on a 71-year-old male patient (flexible bronchoscope).

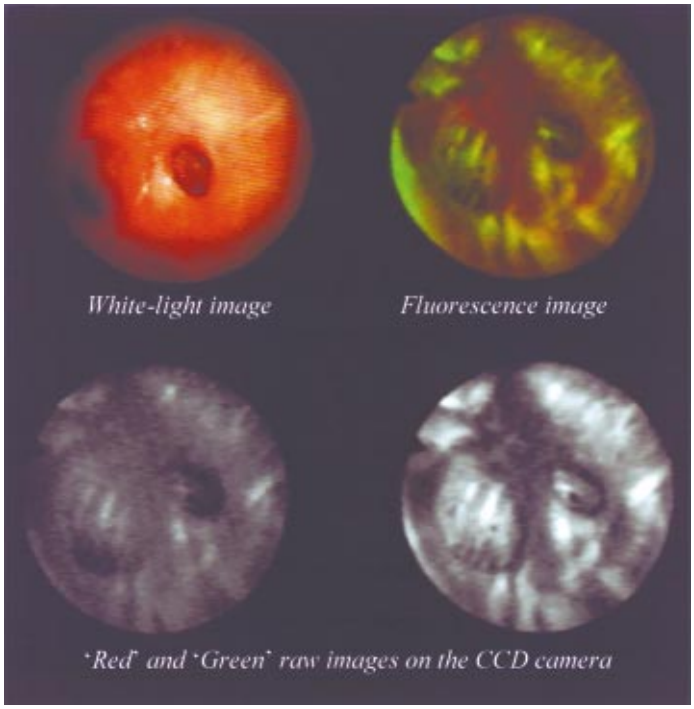

Fig. 6 Photodetection of a moderate dysplasia on a 71-year-old male patient (flexible bronchoscope).

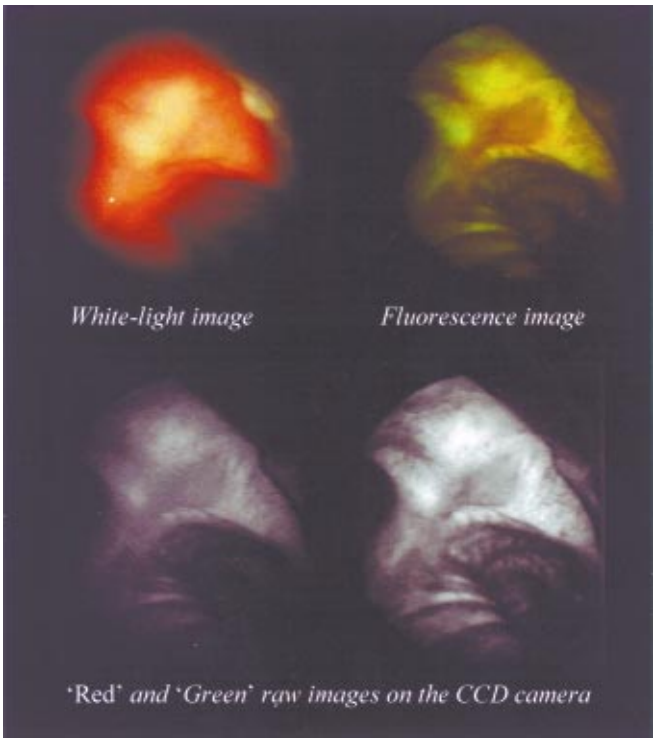

Fig. 7 Photodetection of a hyperplasia on a 61-year-old male patient (rigid bronchoscope).

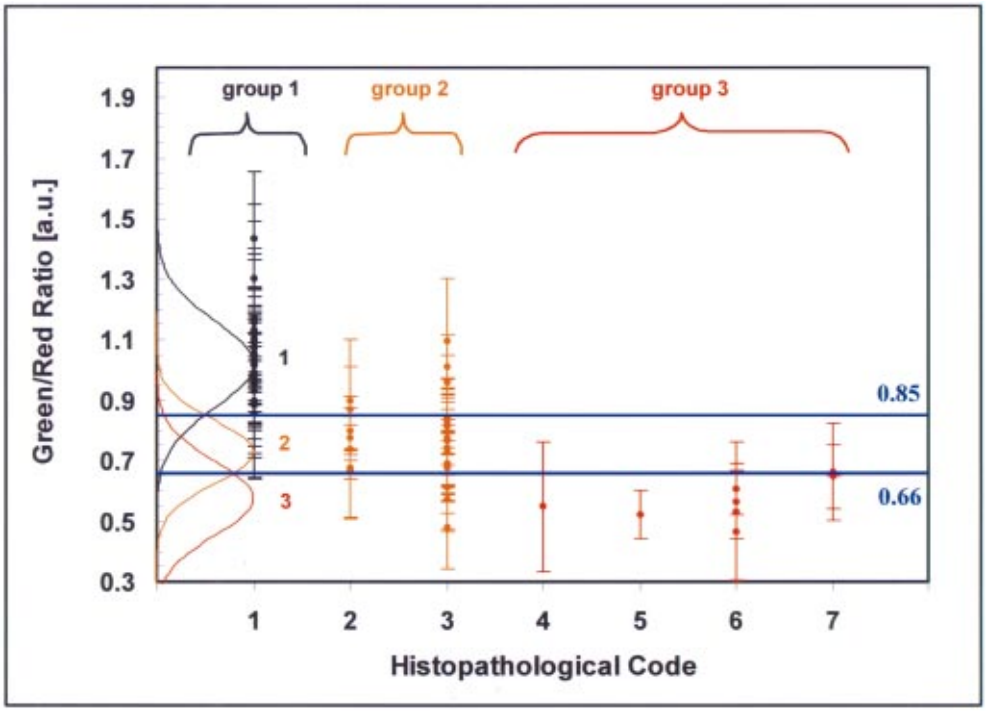

Fig. 8 Green to red ratio of the healthy group (curve 1, group 1), the nonhealthy group (metaplastic/inflammatory: curve 2, group 2), and of the cancer group (malignant: curve 3, group 3) tissues as a function of the histopathological status (see Table 1). The errors bars represent the 67% confidence interval. The curves on the left axis are the projected normal distribution curves corresponding to the green/red ratios.

Table 2 Results of the PPV analysis after application of the decision threshold.

	True Positive (TP)	False Positive (FP)	PPV
AF	9 (AF only=4)	3 (AF only=3)	75%
WL	5 (WL only=0)	8 (WL only=8)	39%

Number of patients=15; number of biopsies=20; AF=autofluorescence mode; WL=white light mode; PPV=TP/(TP+FP) with TP=true positive results and FP=false positive results.

biopsy (lobectomy scar, Figure 5) confirmed the presence of an infiltrating little-differenciated epidermoid carcinoma. Note that this site appeared erythroplasic under WL illumination. The second biopsy (on the site of the PDT, Figure 6) was analyzed as a moderate dysplasia. This site appeared also suspicious in WL mode, but the AF mode enabled us to clearly see the delineation of the suspicious area. This enabled us to retreat precisely this area by PDT, as the previous treatment had probably been underestimated.

3.2 Overall Results

Thirty-three biopsies altogether were taken on sites that were suspicious (positives) during visual inspection of the bronchi in AF or WL modes on the 20 patients involved in this study. Nine of them were confirmed to be true AF positives by histopathological analysis. Thirteen of these 33 sites were positive in WL mode, whereas only 5 of them turned out to be true positives. The qualitative nature of the visual inspection in AF as well as in WL modes has the consequence that the number of false positives depends on the physician's learning curve. Therefore, we added the aforementioned decision thresholds as a quantitative measure to reduce the number of false positives in AF mode. After the application of this criterion, only 12 of the 33 biopsies remained positive, thus 21 of the 24 false positives could be rejected. Together with the WL positives, a number of 20 biopsies taken on 15 patients remained for further analysis. The performance of AF and WL endoscopy on the remaining 20 positive sites are summarized in Table 2.

Note that the hyperplasia presented in Figure 7 gives a normalized green/red ratio of 0.74 ± 0.04 and is consequently rejected with this method.

The PPV gives the probability that a lesion is actually a lesion if visible with a given method (AF or WL), as opposed to the sensitivity that gives the capability of a method to find a lesion if there actually is a lesion. The PPV value is given as the ratio of the true positive (TP) results on the overall positive results [true and false positive (FP)].

The three false positive results remaining in AF mode after the threshold approach were not positive in the WL mode. This means that if we combine the AF thresholding mode with the WL mode, the resulting PPV is 100%.

Note that four lesions were detected by AF only, whereas no lesions were detected by WL only. This means that the AF sensitivity ($SENS_{AF}$) is higher than the WL sensitivity ($SENS_{WL}$). Although it is not possible to calculate a value for $SENS_{AF}$ (as the false-negative rate is not measurable in this organ),[3] one can nevertheless estimate this parameter from $SENS_{WL}$ by the expression $SENS_{AF} = SENS_{WL}(TP_{AF}/TP_{WL})$, where TP_{AF} and TP_{WL} are the true-positive results under AF and WL, respectively. This leads to a $SENS_{AF}$ 1.8 times higher than $SENS_{WL}$ (Table 2).

4 Discussion

AF photodetection has been proven to be a useful tool in detecting early stage lesions in selected cases in the past. Our system is an attempt at improving the AF photodetection method using improved spectroscopy and quantitative decisional functions. The necessity to take full advantage of the potentialities of AF photodetection as an early lung cancer detection method becomes more and more important as the screening of high-risk patient groups makes significant advances. Currently, spiral computer tomography, sputum cytology of a marker as monoclonal antibody A2/B1, proteomic or genomic alterations are novel, promising patients screening methods that are of great interest to be used in combination with our system. Nevertheless, sputum cytology is currently the only clinically approved sputum test for detecting lung cancer, and note that the quality of the expectorations plays a major role on the sensitivity and the specificity of this low-cost screening method.

The preliminary clinical results presented in this paper are very encouraging and illustrate the importance of conducting a spectroscopic analysis[1] before designing such an imaging AF detection apparatus. Moreover, a PPV of 75% for AF mode only can be reached using decision thresholds. This number is large as compared to the LIFE (Xillix) or SAFE (Pentax) systems for which[8,9] the corresponding PPVs do not exceed 40%. Note that the comparison of these numbers must be performed with caution as the prevalence was not exactly the same in these studies.

It is interesting to note that the quantification of the green/red ratio leads to a better discrimination of the results as the positivity criterion is objective. This means that the setting up of an objective threshold is necessary to take full advantage of the method, as long as the endoscopist did not reach his learning curve. This ratio calculation, which was performed offline up to now, can easily be implemented online, as the computational treatment is simple and quick, using a frame-grabbing unit and standard imaging software. This will represent a real-time diagnosis method, and will also have the advantage to bring the endoscopist to his optimal learning curve with more efficacy.

Note that the choice of the decision thresholds must be optimized, depending on the sensitivity and specificity requirements. For example, the thresholds could be adjusted to reach a better sensitivity, which will be detrimental to the specificity, the latter being compensated by the use of a spectrofluorometer (like the one we used to optimize the spectral design[1]) in combination with our system. Indeed, it is likely that a PPV of 100% for the combined approach (AF+WL) could be maintained even if the threshold defined earlier is reduced.

As we can see in Figure 8, the overlap of the three distributions is nonnegligible. One reason for this is the relatively small number of patients, which should be increased in a more extended study. Nevertheless, the intrinsic width of

these distributions can be decreased if the contrast between healthy and diseased tissue can be increased.

One possible method would be to use additional red backscattered light as a constant background to generate the contrast from green AF variation with respect to this additional light and not to red AF, which also presents a decrease of intensity associated with the presence of a lesion. Using an optimized amount of red backscattered light, the contrast can be increased by a factor two, according to M. Zellweger et al.[1]

The choice of backscattered red light appears to be a sensible spectral choice as it should not interfere with changes of tissue optical properties. In this respect, the choice by Storz[6] to use backscattered blue light might prove a bit disappointing as blue light will be absorbed by the blood. It will consequently appear dark and possibly generate false positive results. Another possibility to enhance the contrast is to use a narrower excitation wavelength band (currently 80 nm), as we found[1] that the contrast has its maximum at 405 nm.

The use of these quantitative decision functions as an objective criterion, and the ability to do so in real time in the endoscopy room is of major importance according to our preliminary results. Using this approach, the number of false positive results can be cut down to a low level. Moreover, it is also clear that the AF detection contributes to the localization of early cancerous lesions that would otherwise be missed by the endoscopist, as we can see in Table 2.

References

1. M. Zellweger, P. Grosjean, D. Goujon, Pr. Monnier, H. van den Bergh, and G. Wagnieres, ''*In vivo* autofluorescence spectroscopy of human bronchial tissue to optimize the detection and imaging of early cancers,'' *J. Biomed. Opt.* **6**(1), 41–52 (2001).
2. J. Hung, S. Lam, J. C. LeRiche, and B. Palcic, ''Autofluorescence of normal and malignant bronchial tissue,'' *Lasers Surg. Med.* **11**, 99–105 (1991).
3. G. Wagnières, W. Star, and B. Wilson, ''*In vivo* fluorescence spectroscopy and imaging for oncological applications,'' *Photochem. Photobiol.* **68**(5), 603–632 (1998).
4. R. Richards-Kortum and E. Sevick-Muraca, ''Quantitative optical spectroscopy for tissue diagnosis,'' *Annu. Rev. Phys. Chem.* **47**, 555–606 (1996).
5. Pentax SAFE-1000, *Technical Data*, Description leaflet (2000).
6. M. Leonhard, ''New incoherent autofluorescence/fluorescence system for early detection of lung cancer,'' *Diagnostic Therapeutic Endosc.* **5**, 71–75 (1999).
7. A. Radu, P. Grosjean, C. Fontolliet, G. Wagnieres, A. Woodtli, H. van den Bergh, and Pr. Monnier, ''Photodynamic therapy for 101 early cancers of the upper aerodigestive tract, the esophagus and the bronchi: a single-institution experience,'' *Diagnostic Therapeutic Endosc.* **5**, 145–154 (1999).
8. S. Lam, M. Unger, V. Rush, and J. C. LeRiche, ''Localization of bronchial intraepithelial neoplastic lesions by fluorescence bronchoscopy,'' *Chest* **113**(3), 696–702 (1998).
9. T. Horvath, M. Horvathova, F. Salajka, et al., ''Detection of bronchial neoplasia in uranium miners by autofluorescence endoscopy (SAFE 1000),'' *Diagnostic Therapeutic Endosc.* **5**, 91–98 (1999).